



Formation mechanism of the solid electrolyte interphase in different ester electrolytes†

Cite this: *J. Mater. Chem. A*, 2021, 9, 19664Received 30th March 2021
Accepted 19th May 2021

DOI: 10.1039/d1ta02615a

rsc.li/materials-a

The solid electrolyte interphase (SEI) plays a critical role in determining the performance of lithium metal batteries. Herein, the formation mechanisms of the SEI is investigated in electrolytes with two frequently adopted solvents: diethyl carbonate (DEC) and ethylene carbonate (EC). The dispersity of reaction products between Li and solvents are explored by ¹H-NMR and first-principles calculations. Lithium ethylene carbonate (LEC), the reduction product of DEC, disperses in the electrolyte, while lithium ethylene dicarbonate (LEDC), the reduction product of EC, cannot disperse in the electrolyte. First-principles calculations further prove that the low polymerization degree of (LEC)_n leads to its good dispersity, while poly-LEDC macromolecules can remain on the Li surface acting as the stable SEI. This work not only clearly points out the formation mechanism of SEI, but also demonstrates the functional role of EC, which can provide novel insights for electrolyte design of advanced batteries.

High energy density is the perpetual motivation for advanced battery systems, which requires continuous innovations in electrode materials.^{1–8} Since 1960s, the lithium (Li) metal anode has attracted widespread interest due to its ultra-high theoretical specific capacity (3860 mA h g⁻¹) and the most negative electrode potential (−3.04 V vs. the standard hydrogen electrode).^{9–16} Two main problems hinder the practical applications of rechargeable Li metal batteries: Li dendrite growth and the highly reactive nature of Li metal.^{17,18} The formation of a stable

solid electrolyte interphase (SEI) on the Li anode is considered as an important solution to handle these problems.^{19,20}

During the last four decades, several novel strategies have been proposed to induce the formation of a stable SEI on the Li metal anode, including electrolyte modifications^{21–25} and ex situ SEI design.^{26–29} Previous research studies have found that Li deposition in cyclic carbonate (such as ethylene carbonate (EC) and propylene carbonate (PC)) exhibits better uniformity and compactness than that in linear carbonate (such as diethyl carbonate (DEC), dimethyl carbonate (DMC), and ethyl methyl carbonate (EMC)).^{30,31} The nature of electrolytes is generally related to the deposition morphology of Li by forming a “good” SEI. However, most of the understanding on the SEI and the design principles of it are very empirical due to the little knowledge on the SEI formation mechanism and its exact structure. Therefore, it's of vital importance to clearly understand how SEI forms on the Li anode.

Herein, the formation mechanisms of SEI in different electrolytes (1.0 M LiPF₆-DEC, 1.0 M LiPF₆-EC, and 1.0 M LiPF₆-EC/DEC (1 : 1 by vol)) were investigated. A Li|Cu cell in 1.0 M LiPF₆-DEC exhibits the lowest coulombic efficiency (CE) than in the rest of the electrolytes, which is caused by the different dispersities of reaction products between Li and solvents. Li ethyl carbonate (LEC) formed by the reduction of DEC indicates the high dispersion in the electrolyte, resulting in no SEI formation in the DEC-based system. The apparent Tyndall Effect confirms the colloidal nature of the reacted solution. In contrast, Li ethylene di-carbonate (LEDC), the reduction product of EC, cannot be well distributed in the solution and thus forms a robust SEI which prevents the continuous reaction between EC and Li. First-principles calculations further demonstrate that the formation mechanism of SEI was decided by the different dispersities of the two products. It is quite difficult to achieve the further growth of (LEC)₂; as a result, (LEC)_n with low polymerization will disperse in the solution and form a colloid. In contrast, (LEDC)_n tends to grow continuously and eventually forms poly-LEDC acting as the SEI on the surface of Li.

^aSchool of Materials Science & Engineering, Beijing Institute of Technology, Beijing 100081, China

^bBeijing Key Laboratory of Green Chemical Reaction Engineering and Technology, Department of Chemical Engineering, Tsinghua University, Beijing 100084, China. E-mail: cxb12@mails.tsinghua.edu.cn

^cAdvanced Research Institute of Multidisciplinary Science, Beijing Institute of Technology, Beijing 100081, China

† Electronic supplementary information (ESI) available: Experimental procedures, first-principles calculation details, battery cycling performance (S1 and S5), electrolytic cell's image (S2 and S6), solutions' images (S3, S7 and S8), SEM photos (S4), binding energy between Li⁺ and anions (S9), extended experiments of FEC and DMC (S10). See DOI: 10.1039/d1ta02615a

As a classical experimental system, Li|Cu cells were employed to investigate the Li utilization during Li plating and stripping processes, which can indicate the stability of the SEI. The electrochemical performance of Li|Cu electrolytic cells with extremely excessive electrolyte (20 mL) were studied in different electrolytes (Fig. 1a). For 1.0 M LiPF₆-DEC, the extremely low CE indicates that deposited Li cannot be stripped from the Cu current collector (Fig. S1†), while no Li remains on the Cu foil (Fig. 1b). For 1.0 M LiPF₆-EC and 1.0 M LiPF₆-EC/DEC, improved CEs can be obtained. It is worth mentioning that in 1.0 M LiPF₆-EC, the CE of the battery decreases because the electrolyte gradually solidifies during the testing process due to its extremely high melting point of EC (~36 °C).³² Though the melting point of the EC solvent itself is higher than room temperature, the fresh 1.0 M LiPF₆-EC electrolyte is a liquid because the addition of LiPF₆ decreases the melting point of the electrolyte. The increase in CE for the 1.0 M LiPF₆-EC electrolyte from the first to third cycle is caused by Li consumption during SEI formation. The thick Li deposition layer observed with the 1.0 M LiPF₆-EC electrolyte is caused by the accumulation of the large amount of “dead” Li and severe volume change in the pressure-free electrolytic cells. After adding DEC as a co-solvent with a lower melting point and viscosity, the CE of the Li|Cu cell has taken a leap forward. A large amount of residual Li on the surface of Cu foil after cycles can also be observed in the 1.0 M LiPF₆-EC and 1.0 M LiPF₆-EC/DEC electrolytes (Fig. 1c and d).

The colour of the cycled 1.0 M LiPF₆-DEC electrolyte changes severely, while those of cycled 1.0 M LiPF₆-EC and 1.0 M LiPF₆-EC/DEC electrolytes remain nearly the same during cycling (Fig. S2 and S3a†). To avoid the effect of floating dead Li in the cycled electrolytes, methanol-D (CD₃OH) was used to consume the Li in different solutions. 1.0 M LiPF₆-DEC solution still appeared brown, whereas the others became slightly transparent, indicating that large floating Li existed in the cycled

1.0 M LiPF₆-EC and 1.0 M LiPF₆-EC/DEC electrolytes, while additional products existed in the cycled 1.0 M LiPF₆-DEC electrolyte (Fig. S3†). Therefore, a stable SEI can be obtained in the EC-based electrolyte, but an unstable interface occurs on the Li metal anode for the DEC-based electrolyte. It is forecasted that decomposing products of the EC-based electrolyte can be deposited on the electrode as a stable SEI, while the decomposing products of the DEC-based electrolyte is distributed in the electrolyte and cannot form a stable SEI to reduce the continuous reactions between deposited Li and the electrolytes. The corresponding SEM images also show that there are no Li deposits on the surface of copper foil in the 1.0 M LiPF₆-DEC electrolyte, while similar Li deposits are observed in the 1.0 M LiPF₆-EC or EC/DEC electrolyte (Fig. S4†).

LiPF₆ is reported to exhibit poor stability against Li.^{29,33} Li bis((trifluoromethyl)sulfonyl)azanide (LiTFSI) was used for further verification of the roles of solvents in order to get rid of the impact of LiPF₆, (Fig. S5†). Similarly, the near to zero CE in the 1.0 M LiTFSI-DEC electrolyte shows that deposited Li cannot be stripped from the Cu current collector, and no Li remains on the Cu foil (Fig. S5b†). But in the 1.0 M LiTFSI-EC or EC/DEC electrolyte, elevated CE is obtained and deposited Li remains on the Cu foil (Fig. S5c and d†). The 1.0 M LiTFSI-DEC electrolyte is found to be brown, while the others are still clear (Fig. S6†). After using CD₃OH to consume the floating Li in the electrolyte, the solution of 1.0 M LiTFSI-DEC still appears brown, showing that new products exist in the cycled 1.0 M LiTFSI-DEC electrolyte (Fig. S7†). However, the others become slightly transparent, indicating that there is only floating Li existing in the electrolyte (Fig. S7†). This phenomenon has proved that the decomposition products of the DEC or EC solvent are independent of Li salt.

The decomposing products between EC, DEC and Li metal were analysed to investigate the generation of SEI. The main purpose of using 60 °C as the reaction temperature of Li and solvents is to make sure that EC is liquid and can react with Li adequately. Li can continuously react with DEC and the Tyndall Effect of the solution indicates that the reaction product can disperse in the solution easily and appears colloidal in nature (Fig. 2a). Therefore, no effective SEI can be formed on the surface of Li in the DEC solvent. In contrast, when EC is the solvent or co-solvent, the reaction between Li and EC is quite mild and self-limited, and Li is still crushed into particles and suspended in the solution (Fig. 2b and c). Then, CD₃OH was added into the suspension liquid. It was found that the solution became clear, which means that large amounts of Li were consumed (Fig. S8b and c†).

¹H-NMR was employed to further probe the reaction products in the solutions. It has been reported that the major products of reactions between DEC and Li is LEC and it exhibits two hydrogen peaks at 3.6 and 1.1 PPM, which can be identified from Fig. 2d clearly.^{34–36} The main product of reactions between EC and Li is LEDC and it exhibits a hydrogen peak at 3.5 PPM, which cannot be observed in Fig. 2e and f.^{36–39} These results indicate that LEC can be distributed in the electrolytes easily, while LEDC is deposited on the Li metal anode and can be reduced to more stable compounds gradually (Li₂O, Li₂CO₃,



Fig. 1 Electrochemical performance of the Li–Cu electrolytic cell with different electrolytes (1.0 M LiPF₆-DEC, EC and EC/DEC (1 : 1 by vol)). (a) Coulombic efficiency in different electrolytes. The inset photo shows the assembled electrolytic cell. Plated Li morphology in various electrolytes: (b) 1.0 M LiPF₆-DEC, (c) 1.0 M LiPF₆-EC, and (d) 1.0 M LiPF₆-EC/DEC (1 : 1 by vol). Due to the continuous reactions between Li and DEC, there is no Li residue on Cu foil for (b), while large amounts of Li remain on Cu foil on account of the self-limiting reactions between Li and EC in (c and d).

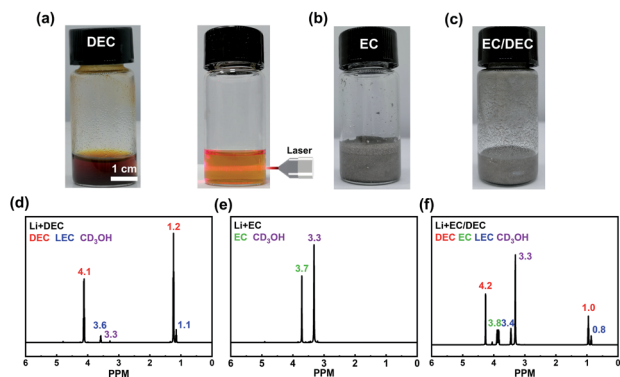


Fig. 2 Reactions between Li and different solvents. Optical images of the solutions of Li with different solvents: (a) DEC, (b) EC, and (c) EC/DEC (1 : 1 by vol) after stirring at 60 °C for 4 days. The Tyndall Effect of the solution with DEC after being diluted by DEC (right panel of (a)) indicates that the reaction products of Li and DEC are colloidal and exhibit high dispersity in the solvents, maintaining stability for 14 days. Corresponding $^1\text{H-NMR}$ spectra of the reaction products of Li and (d) DEC, (e) EC, and (f) EC/DEC (1 : 1 by vol) after stirring at 60 °C for 4 days. The LEC reaction products of Li and DEC can be detected in the solution, while the LEDC reaction products of Li and EC cannot be detected in the solution, indicating that the reaction between Li and DEC is not self-limited and the reaction between Li and EC is self-limited.

etc.).^{40,41} Therefore, two completely different scenarios appear: The reactions between DEC and Li metal cannot form a self-limited SEI, while EC can render a stable SEI on the Li metal anode.

Theoretical calculations were further conducted to afford a deeper understanding towards the formation mechanism of SEI. The binding strength between reaction products and solvent molecules can be thought to be a reflection of their dispersity. The binding energy between Li cations in LEC or LEDC and anions are extremely high (−3.25 and −3.20 eV, respectively) compared with that between Li cations and DEC or EC solvents (−1.15 and −0.67 eV, respectively) (Fig. S9†). Hence, LEC and LEDC tend to exist as whole molecules instead of dissociating into cations and anions.

The interactions of LEC and LEDC with themselves and solvents are further studied. For the DEC electrolyte system, the binding energy between LEC and LEC molecules (LEC–LEC) is the strongest (−2.39 eV) compared with those of LEC–DEC, (LEC)₂–LEC, and (LEC)₂–(LEC)₂ (Fig. 3a), indicating that LEC molecules tend to connect in pairs, which is similar to the conclusion of previous research.⁴² Subsequently, two (LEC)₂ molecules can continue to combine with LEC or (LEC)₂ and form (LEC)_{3/4}, with the decrease of binding energy (−2.02 and −1.75 eV, respectively). Besides, the closed-loop system of (LEC)₄ hinders its further growth (Fig. 3b). (LEC)₂ and (LEC)₄ with low polymerization degrees readily disperse in solvents and cannot restrain the continuous reaction of Li metal and the electrolyte. Besides, the relatively large molecular volume of (LEC)₂ and (LEC)₄ render the solution colloidal properties (Tyndall Effect in Fig. 2a). In contrast, LEDCs exhibit a chain growth pattern into large polymers with no binding energy

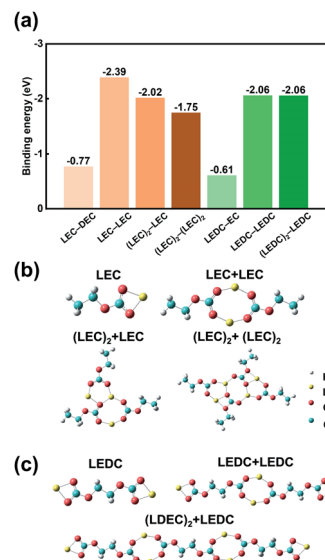


Fig. 3 Binding features between different LEC and LEDC molecules. (a) Binding energies between LEC or LEDC molecules and the corresponding binding form in (b) and (c). LEC and LEDC have higher binding energies with themselves compared with these of solvent molecules. LECs can bind together with a decrease of binding energy, whereas LEDCs can grow linearly with no reduction of binding energy.

decrease after successive binding with other LEDC molecules (−2.06 eV) (Fig. 3a and c). This (LEDC)_n polymer has a large molecular volume and cannot be distributed in the electrolyte, thus producing a polymer film on the Li metal anode and acting as a stable SEI.³² The formed SEI can prevent further reactions between Li and the electrolyte, promoting the performance of Li metal batteries in EC based electrolytes.

Extended experiments were conducted to verify the impact of SEI dispersibility on the Li anode with similar solvents. FEC is a cyclic molecule and its reduction path is similar to EC after the loss of a fluorine atom.^{43,44} Li reacts with FEC by heating and stirring; the reactions are quite limited and the Li bulk still keeps its shape (Fig. S10a†). The $^1\text{H-NMR}$ spectrum of the corresponding solution exhibits no signal except for those of FEC and CD₃OH (Fig. S10b†), meaning that the reaction products of FEC and Li metal cannot be well distributed in the solvents. In contrast, it is deposited on the surface of Li metal and acts as a self-limiting layer to stop further reactions. Dimethyl carbonate (DMC) is another famous linear molecule similar to DEC.^{45,46} After stirring DMC and Li at an elevated temperature, CD₃OH was used for the consumption of the remaining Li in the solution. The Tyndall Effect also appears for the residual solution, revealing that Li methyl carbonate (LMC), the reaction product of Li and DMC, has good dispersibility in the solution (Fig. S10c†). In addition, the characteristic peak of LMC at 3.7 PPM can be seen in the $^1\text{H-NMR}$ spectrum of the corresponding solution (Fig. S10d†).³⁶ Two LMCs will combine together,⁴² forming a colloid like LEC.

Based on the analyses above, the dispersibility of reaction products between Li and solvents will affect the stability of the interface of the Li metal anode (Fig. 4) and finally the



Fig. 4 Scheme of SEI formation in different electrolytes. Ester linear molecules like DEC and DMC react with Li, forming well dispersed polymers with short chains and leading to an unstable interface between the Li metal anode and the electrolyte. However, cyclic molecules like EC and FEC react with Li, forming polymers with long chains, which can remain on the surface of the Li metal anode and act as a stable SEI.

electrochemical performance of batteries dramatically. Ester linear molecules, such as DEC and DMC cannot form a stable SEI on the Li surface and will corrode Li metal steadily owing to the high dispersion of the decomposing products. As a result, Li metal batteries cannot work efficiently in 1.0 M LiPF₆-DEC. Contrarily, cyclic molecules, such as EC and FEC, can generate a layer deposited on the surface of Li, guaranteeing that the side reaction is self-limited. Therefore, the consumption of Li and the electrolyte is greatly reduced, resulting in higher CE in 1.0 M LiPF₆-EC and 1.0 M LiPF₆-EC/DEC.

In conclusion, the formation mechanisms of SEI in different electrolytes were comprehensively investigated by employing EC and DEC as two typical solvents. The dispersibility of reaction products in solvents and Li metal has a significant role in the SEI formation. The CE of the Li|Cu cell in 1.0 M LiPF₆-DEC is extremely low, because LEC generated by the reaction of Li and DEC can disperse in the solution easily and cannot form a self-limited SEI film. In contrast, EC as a solvent or co-solvent can react with Li and generate LEDC which cannot disperse in the electrolyte and acts as a stable component of SEI on Li metal. First-principles calculations further unravel the origin of the different dispersibilities of LEC and LEDC. Compared with LEDC, LECs have a lower tendency to aggregate. Therefore, (LEC)_n with low polymerization disperses in the electrolyte and cannot form a SEI on the Li anode. LEDC, the decomposition product of EC, can grow linearly to generate a poly-LEDC film acting as the SEI on the Li surface. This contribution not only indicates the important role of product dispersibility in SEI stability, but also emphasizes the importance of SEI on electrochemical performances. Design principles to regulate SEI can be obtained by investigating the dispersibility of solvent decomposing products.

Conflicts of interest

There are no conflicts to declare.

Acknowledgements

This work was supported by the National Natural Science Foundation of China (21805161, 21808121, and U1932220), China Post-Doctoral Science Foundation (2020M670155 and

2020T130054). The authors acknowledge support from Tsinghua National Laboratory for Information Science and Technology for theoretical simulations.

Notes and references

- M. Li, J. Lu, Z. Chen and K. Amine, *Adv. Mater.*, 2018, **30**, 1800561.
- Z. Li, Q. He, C. Zhou, Y. Li, Z. Liu, X. Hong, X. Xu, Y. Zhao and L. Mai, *Energy Storage Materials*, 2021, **37**, 40–46.
- P. Shi, X. B. Cheng, T. Li, R. Zhang, H. Liu, C. Yan, X. Q. Zhang, J. Q. Huang and Q. Zhang, *Adv. Mater.*, 2019, **31**, 1902785.
- M. S. Whittingham, *Proc. IEEE.*, 2012, **100**, 1518–1534.
- J. F. Ding, R. Xu, C. Yan, B. Q. Li, H. Yuan and J. Q. Huang, *J. Energy Chem.*, 2021, **59**, 306–319.
- Y. Qiao, Q. Li, X. B. Cheng, F. Liu, Y. Yang, Z. Lu, J. Zhao, J. Wu, H. Liu, S. Yang and Y. Liu, *ACS Appl. Mater. Interfaces*, 2020, **12**, 5767–5774.
- M. A. Hope, B. L. D. Rinkel, A. B. Gunnarsdottir, K. Marker, S. Menkin, S. Paul, I. V. Sergeev and C. P. Grey, *Nat. Commun.*, 2020, **11**, 2224.
- F. Wu, J. Maier and Y. Yu, *Chem. Soc. Rev.*, 2020, **49**, 1569–1614.
- B. D. Adams, J. Zheng, X. Ren, W. Xu and J. G. Zhang, *Adv. Energy Mater.*, 2018, **8**, 1702097.
- X. Cao, X. Ren, L. Zou, M. H. Engelhard, W. Huang, H. Wang, B. E. Matthews, H. Lee, C. Niu, B. W. Arey, Y. Cui, C. Wang, J. Xiao, J. Liu, W. Xu and J. G. Zhang, *Nat. Energy*, 2019, **4**, 796–805.
- X. B. Cheng, C. Yan, X. Q. Zhang, H. Liu and Q. Zhang, *ACS Energy Lett.*, 2018, **3**, 1564–1570.
- Z. D. Hood, X. Chen, R. L. Sacci, X. Liu, G. M. Veith, Y. Mo, J. Niu, N. J. Dudney and M. Chi, *Nano Lett.*, 2021, **21**, 151–157.
- S. Nanda and A. Manthiram, *Adv. Energy Mater.*, 2021, **11**, 2003293.
- X. Q. Xu, R. Xu, X. B. Cheng, Y. Xiao, H. J. Peng, H. Yuan and F. Liu, *J. Energy Chem.*, 2021, **56**, 391–394.
- L. Shi, S. M. Bak, Z. Shadike, C. Wang, C. Niu, P. Northrup, H. Lee, A. Y. Baranovskiy, C. S. Anderson, J. Qin, S. Feng, X. Ren, D. Liu, X. Q. Yang, F. Gao, D. Lu, J. Xiao and J. Liu, *Energy Environ. Sci.*, 2020, **13**, 3620–3632.
- C. Sun, A. Lin, W. Li, J. Jin, Y. Sun, J. Yang and Z. Wen, *Adv. Energy Mater.*, 2019, **10**, 1902989.
- H. Liu, X. B. Cheng, R. Xu, X. Q. Zhang, C. Yan, J. Q. Huang and Q. Zhang, *Adv. Energy Mater.*, 2019, **9**, 1902254.
- S. C. Nagpure, T. R. Tanim, E. J. Dufek, V. V. Viswanathan, A. J. Crawford, S. M. Wood, J. Xiao, C. C. Dickerson and B. Liaw, *J. Power Sources*, 2018, **407**, 53–62.
- C. Fang, J. Li, M. Zhang, Y. Zhang, F. Yang, J. Z. Lee, M. H. Lee, J. Alvarado, M. A. Schroeder, Y. Yang, B. Lu, N. Williams, M. Ceja, L. Yang, M. Cai, J. Gu, K. Xu, X. Wang and Y. S. Meng, *Nature*, 2019, **572**, 511–515.
- Z. Luo, X. Qiu, C. Liu, S. Li, C. Wang, G. Zou, H. Hou and X. Ji, *Nano Energy*, 2021, **79**, 105507.

- 21 J. Fu, X. Ji, J. Chen, L. Chen, X. Fan, D. Mu and C. Wang, *Angew. Chem., Int. Ed.*, 2020, **59**, 22194–22201.
- 22 C. C. Su, M. He, R. Amine, Z. Chen, R. Sahore, N. Dietz Rago and K. Amine, *Energy Storage Materials*, 2019, **17**, 284–292.
- 23 S. Li, Z. Luo, L. Li, J. Hu, G. Zou, H. Hou and X. Ji, *Energy Storage Materials*, 2020, **32**, 306–319.
- 24 F. M. Weber, I. Kohlhaas and E. Figgemeier, *J. Electrochem. Soc.*, 2020, **167**, 140523.
- 25 S. Jurng, Z. L. Brown, J. Kim and B. L. Lucht, *Energy Environ. Sci.*, 2018, **11**, 2600–2608.
- 26 S. Liu, J. Luo, L. Jingyue, L. Dai, L. Wang, X. Zhang and Q. Zhao, *J. Mater. Chem. A*, 2020, **8**, 17415–17419.
- 27 M. L. Meyerson, P. E. Papa, A. Heller and C. B. Mullins, *ACS Nano*, 2021, **15**, 29–46.
- 28 J. Yun, B. K. Park, E. S. Won, S. H. Choi, H. C. Kang, J. H. Kim, M. S. Park and J. W. Lee, *ACS Energy Lett.*, 2020, **5**, 3108–3114.
- 29 Y. Liu, R. Tao, S. Chen, K. Wu, Z. Zhong, J. Tu, P. Guo, H. Liu, S. Tang, J. Liang and Y. C. Cao, *J. Power Sources*, 2020, 477.
- 30 Q. Li, Z. Cao, W. Wahyudi, G. Liu, G. T. Park, L. Cavallo, T. D. Anthopoulos, L. Wang, Y. K. Sun, H. N. Alshareef and J. Ming, *ACS Energy Lett.*, 2020, **6**, 69–78.
- 31 F. Ding, W. Xu, X. Chen, J. Zhang, M. H. Engelhard, Y. Zhang, B. R. Johnson, J. V. Crum, T. A. Blake, X. Liu and J. G. Zhang, *J. Electrochem. Soc.*, 2013, **160**, A1894–A1901.
- 32 K. Xu, *Chem. Rev.*, 2004, **104**, 4303–4417.
- 33 S. E. Sloop, J. K. Pugh, S. Wang, J. B. Kerr and K. Kinoshita, *Electrochem. Solid-State Lett.*, 2001, **4**, A42.
- 34 D. Aurbach, M. L. Daroux, P. W. Faguy and E. Yeager, *J. Electrochem. Soc.*, 1987, **134**, 1611–1620.
- 35 L. J. Rendek, G. S. Chottiner and D. A. Scherson, *J. Electrochem. Soc.*, 2002, **149**, E408.
- 36 K. Xu, G. V. Zhuang, J. L. Allen, U. Lee, S. S. Zhang, P. N. Ross, Jr. and T. R. Jow, *J. Phys. Chem. B*, 2006, **110**, 7708–7719.
- 37 T. Liu, L. Lin, X. Bi, L. Tian, K. Yang, J. Liu, M. Li, Z. Chen, J. Lu, K. Amine, K. Xu and F. Pan, *Nat. Nanotechnol.*, 2019, **14**, 50–56.
- 38 M. J. Boyer and G. S. Hwang, *J. Phys. Chem. C*, 2019, **123**, 17695–17702.
- 39 D. M. Seo, D. Chalasani, B. S. Parimalam, R. Kadam, M. Y. Nie and B. L. Lucht, *ECS Electrochem. Lett.*, 2014, **3**, A91–A93.
- 40 A. Ramasubramanian, V. Yurkiv, T. Foroozan, M. Ragone, R. Shahbazian-Yassar and F. Mashayek, *ACS Appl. Energy Mater.*, 2020, **3**, 10560–10567.
- 41 T. Yoon, M. S. Milien, B. S. Parimalam and B. L. Lucht, *Chem. Mater.*, 2017, **29**, 3237–3245.
- 42 L. Wang, A. Menakath, F. Han, Y. Wang, P. Y. Zavalij, K. J. Gaskell, O. Borodin, D. Iuga, S. P. Brown, C. Wang, K. Xu and B. W. Eichhorn, *Nat. Chem.*, 2019, **11**, 789–796.
- 43 S. K. Heiskanen, J. Kim and B. L. Lucht, *Joule*, 2019, **3**, 2322–2333.
- 44 K. Kim, I. Park, S. Y. Ha, Y. Kim, M. H. Woo, M. H. Jeong, W. C. Shin, M. Ue, S. Y. Hong and N.-S. Choi, *Electrochim. Acta*, 2017, **225**, 358–368.
- 45 G. Zhuang, Y. Chen and P. N. Ross, *Langmuir*, 1999, **15**, 1470–1479.
- 46 T. Nakajima, Y. Hirobayashi, Y. Takayanagi and Y. Ohzawa, *J. Power Sources*, 2013, **243**, 581–584.